# UNIVERSITY OF BIRMINGHAM

# Extraordinary THz Transmission with a Small Beam Spot

Navarro-Cia, Miguel; Pacheco-Peña, Víctor; Kuznetsov, Sergei A.; Beruete, Miguel

Link to publication on Research at Birmingham portal

**Extraordinary THz Transmission with a Small Beam Spot: the Leaky Wave Mechanism**

*Miguel Navarro-Cía*[*]*, Víctor Pacheco-Peña, Sergei A. Kuznetsov, and Miguel Beruete*[*]

In memoriam of our beloved friend Prof Mario Sorolla Ayza who was the driving force and source of inspiration for this work.

Dr M. Navarro-Cía
School of Physics and Astronomy, University of Birmingham, Birmingham, Edgbaston, B15 2TT, UK
E-mail: m.navarro-cia@bham.ac.uk
Dr. V. Pacheco-Peña
Department of Electrical and Systems Engineering, University of Pennsylvania, Philadelphia, Pennsylvania 19104, USA
Dr. S. A. Kuznetsov
Rzhanov Institute of Semiconductor Physics SB RAS, Novosibirsk Branch "TDIAM,"
Lavrentiev Avenue 2/1, Novosibirsk 630090, Russian Federation
Novosibirsk State University, Pirogova Street 2, 630090 Novosibirsk, Russian Federation
Dr Miguel Beruete
Antennas Group-TERALAB, Universidad Pública de Navarra, Campus Arrosadía, 31006 Pamplona, Spain
Institute of Smart Cities, Public University of Navarra, 31006 Pamplona, Spain
E-mail: miguel.beruete@unavarra.es

The discovery of Extraordinary Optical Transmission (EOT) through patterned metallic foils

in the late 1990s was decisive for the development of plasmonics and cleared the path to

employ small apertures for a variety of interesting applications all along the electromagnetic

spectrum. However, a typical drawback often found in practical EOT structures is their large

size needed to obtain high transmittance peaks. Consequently, practical EOT arrays are

usually illuminated using an expanded (mimicking a plane wave) beam. Here, we show with

numerical and experimental results in the THz range that high transmittance peaks can be

obtained even with a reduced illumination spot exciting a small number of holes, provided

that the structure has a sufficient number of lateral holes out of the illumination spot. These

results shed more light on the prominent role of leaky waves in the underlying physics of EOT and have a direct impact on potential applications.

## 1. Introduction

The phenomenon of Extraordinary Optical Transmission (EOT) through subwavelength apertures perforated on a host metal plate has been crucial for the development of plasmonics, which is now a central part of nanophotonics technology, opening new avenues toward high performance devices such as color filters,[1] sensing platforms,[2] etc. However, a typical drawback of EOT hole arrays compared to other two-dimensional structures such as metasurfaces[3] is the relatively large number of holes necessary to get a well-defined resonance peak with high amplitude.[4] Indeed, this strong dependence of EOT on the number of holes was identified since the first experiments dealing with the phenomenon[5] and was explained invoking surface plasmons. Experimental results at infrared[5] already showed noticeable differences between large and small arrays. More systematic studies dealing with the enhancement of transmission as the size of the array was gradually increased were reported in the millimeter-wave regime[4],[6],[7] and it was found that with 961 holes ($31 \times 31$) total transmission was reached.[7] Afterwards, theoretical[8] and experimental[9] works arrived at the same conclusion.

It is nowadays well-established that the EOT resonance in subwavelength hole arrays (and also in an aperture flanked by periodic corrugations as discussed later) relies on surface electromagnetic modes that arise due to the coupling between holes (whose shape and size modulate slightly the EOT as long as the holes remain subwavelength, i.e., cut-off regime,[4],[7],[10]-[15]), regardless the precise origin of these surface modes.[16]-[24] In real metals at visible frequencies, coupling is possible through surface plasmon polaritons as well as diffraction modes.[22] In contrast, metals at terahertz are generally considered as good conductors, and they fit in a high conductivity model which is a good approximation to a

perfect conductor. In this regime, surface plasmons cannot be supported and all the coupling is through diffraction.[19] Then, the surface modes responsible for the coupling are leaky waves[17],[22],[23],[25]-[27], i.e. complex waves[27] that radiate power away from the surface as they propagate along it. Leaky waves were already invoked in the prominent work by Ulrich[26] to explain the salient features of metal meshes in the far infrared, principally strong peaks in the transmittance that are directly related to the so-called resonant Wood's anomalies of reflection gratings[17],[25],[26] and that emerge as a result of the interference between the direct beam and the leakage beams.

Aside from this, other models have been proposed to explain EOT, which can be classified into three main frames: (i) theory based on surface plasmons,[5],[16],[18] and (ii) full-wave diffraction models[8],[17],[19],[24],[28] discussed above, and (iii) theory based on waveguide and impedance matching, also known as equivalent circuit model.[23],[29] The main merit of the first frame is its simplicity; but, because of that, accurate quantitative predictions are difficult to reach. The second frame is a comprehensive theory that yields accurate quantitative results at the expense of intensive computational efforts. The latter frame, equivalent circuit models, has been championed by the microwave engineering community more recently than the others to ensure accurate quantitative predictions with reduced computational efforts. A common characteristic in all EOT theoretical analyses is that they usually deal with infinite structures and accordingly, experiments use uniform (quasi-plane-wave) illumination to efficiently excite all the apertures in the array.

The aim in this work is twofold: (i) to demonstrate that a high EOT resonance peak is feasible even when a small number of holes are directly illuminated if there is a sufficient number of lateral holes participating in the resonance process (a fact that has been disregarded in previous analytical and experimental studies dealing with EOT in subwavelength hole arrays); (ii) to provide direct evidence of the key role of leaky waves in the EOT resonance.[30],[31]

## 2. Results and Discussion

### 2.1. Illuminated Holes vs. Total Number of Holes: the Leaky Wave Mechanism

To demonstrate the excitation of EOT resonance even with a few illuminated holes, several experiments were performed employing rectangular- and square-lattice subwavelength hole arrays (see **Figure 1**) and four experimental set-ups described in the materials and methods section. The arrays were implemented both in substrate-backed and substrate-free configurations. The geometrical parameters for each sample along with the corresponding EOT resonance frequency can be found in **Table I**. To motivate this study, we first focus on sample I, whose EOT resonance peak takes place at $f = 0.22$ THz ($y$-polarized excitation). Under an expanded beam illumination with an incident beam-waist of $\varpi_0 = 12.5$ mm (i.e., beam diameter of 25 mm and spot area of 490.9 mm$^2$) that illuminates directly 1050 holes ($n_x \times n_y = 50 \times 21$), the peak transmittance reaches 73.2% ($-1.35$ dB, see **Figure 2**). Under a collimated beam illumination with a beam-waist of $\varpi_0 \sim 3$ mm, the peak drops slightly to 64% ($-1.91$ dB), even though the effective illuminated area is just 28.3 mm$^2$ and covers barely 60 holes ($12 \times 5$). This number is well below the reported minimum number of 961 holes ($31 \times 31$) to get noticeable transmission in freestanding EOT plates.[4],[7]-[10] Moreover, although the number of holes with the former set-up is 17.5 times larger (1050 vs 60 holes), the transmittance in both cases differs insignificantly. This result gives a first evidence that a high transmission can be achieved even when the number of directly illuminated holes is extremely small.

An explanation to this, at first sight, unexpected result can be found by recalling the inherent mechanism of EOT. As mentioned in the introduction, the EOT resonance is linked to the excitation of surface electromagnetic modes, which are surface plasmon polaritons combined with diffraction modes in optics[22] and leaky waves at THz[17],[22],[23],[25]-[27],[30],[31]. From this point of view, the physics of the hole array are in essence identical to the conceptually easier

one-dimensional structures analyzed previously,[30],[32],[33] where the transmission through a small aperture was enhanced by corrugating the metallic plane. The underlying mechanism in corrugated structures is also a surface Bloch mode[30] (leaky wave) excited by the periodic structure. By analogy, the tiny aperture of these structures can be identified with the illuminated central part of our hole array and the lateral corrugations with the non-illuminated holes. An interesting particularity of the hole array is that power can be transmitted through every aperture (hence, the aperture size has some effect on the EOT as discussed elsewhere[4],[7],[10],[11],[14]) and, therefore, it is more similar to a configuration with corrugations on the input and output faces, in the sense that the incident power on the input excites the (0, −1) space harmonic, which is a leaky mode that propagates along the hole array, and is coupled to the output face through the apertures. Then, intrinsically there is a leaky wave on the input face and another one on the output face. Under this perspective, the number of holes surrounding the illuminated area become of particular importance, since it has been demonstrated that the leaky wave excited at EOT has a small radiation per unit length and, thus, it can explore a high number of apertures before its power becomes negligible[9],[17],[20],[26],[30],[31]. Once the leaky wave has been excited by direct beam incidence on a set of holes, the surface mode is capable of exploring several adjacent apertures (not directly excited by the incident beam) and, as demonstrated here, a large transmittance is possible with a very reduced number of illuminated holes (12 × 5) as long as there are enough lateral holes. Thus, an obvious distinction arises between effectively illuminated holes and total number of holes. This is the main message of this manuscript.

## 2.2. Number of Holes and beam-waist dependence

As an alternative approach to demonstrate the leaky wave mechanism and the distinction between illuminated and total number of holes, we perform here a systematic analysis by measuring truncated square-lattice subwavelength hole arrays (samples II and III) of different

dimensions (from $1 \times 1$ to $107 \times 107$ ) illuminated with Gaussian beams of different sizes. This study expands previous works dealing with truncated subwavelength hole arrays that considered uniquely uniform illumination (plane wave) neglecting the importance of the number of illuminated holes vs. total number of holes.[6],[7],[21],[34]

**Figure 3a,b** displays the measured and calculated transmission coefficient through sample II illuminated by a focused beam with $\varpi_0 = 1$ mm (panel a) and $\varpi_0 = 5$ mm (panel b). Also, the attenuation with respect to the maximum transmission for each case is shown in **Figure 3c** as a summary (complemented with an additional study considering a beam-waist of 1.5 mm) and to support the discussion. These results demonstrate again that high transmission is feasible even with small number of illuminated holes, provided the array is large enough so that the leaky wave can run through a sufficient number of holes. Notice that transmission is routinely higher for $\varpi_0 = 5$ because of its narrower angular distribution; this is discussed further in the next section.

Let us first concentrate on the incident Gaussian beam with beam-waist $\varpi_0 = 1$ mm (Figure 3a and blue line-triangle in Figure 3c). With this setup, the beam size is equivalent to 16 ($4 \times 4$) holes approximately. For smaller matrices ($1 \times 1$ and $3 \times 3$ holes) the transmission is accordingly small (in these cases there are no lateral holes). However, as soon as there are some lateral holes surrounding the illumination areas, the transmission abruptly increases and the EOT resonance takes a definite shape. In the case of a matrix of size $7 \times 7$ a significantly high transmission (although not maximum) is achieved (3.6 dB insertion loss) with a well-defined resonance. Transmission saturates for the $15 \times 15$ array, whose area is approximately 14 times larger than the beam spot. This reinforces the previous theoretical finding that the leaky wave at EOT has a small radiation per unit length and, thus, it explores a high number of apertures before its power becomes negligible.[9],[17],[20],[26],[30],[31] In brief, saturation is met when the area of the array is significantly larger than the beam spot area ($\pi \cdot \varpi_0^2$).

The same conclusion can be reached from the experiments with beam-waist $\varpi_0 = 5$ mm (Figure 3b and black line-square in Figure 3c) and $\varpi_0 = 1.5$ mm (red line-circle in Figure 3c), where the beam size is respectively equivalent to 400 ($20 \times 20$) and 36 ($6 \times 6$) holes approximately. It is worth noticing that, despite the fact the three curves in Figure 3c correspond to different setups, they have a similar trend and they all indeed suggest that the saturation of the transmission happens when the hole matrix area is approximately 10 times the beam spot. This univocally corroborates the leaky wave mechanism.

Similar to the theoretical results for plane-wave illumination from Ref. [34], we observe that the resonant transmission and Rayleigh-Wood anomaly start to be distinguished for $3 \times 3$ arrays regardless of the beam-waist of the illumination. The need of a certain hole array size for the resonant transmission and the Rayleigh-Wood anomaly is directly related to the leaky wave mode that runs along the hole matrix. This leaky mode channels energy evanescently through the subwavelength aperture while travelling outwards from the beam-spot. A minimum number of holes are needed for the incident beam to couple to the leaky wave and for the leaky wave to transfer all the energy to the second interface, where it is subsequently re-radiated. Once all incident power has been coupled to the second interface and re-radiated there (and absorbed due to conductive and dielectric losses), the rest of outer holes are superfluous.

The above discussion is illustrated in **Figure 4a**, wherein the *E*-field distribution at 0.51 THz is plotted on the *E*-plane for the $107 \times 107$ array under 1 mm beam-waist illumination. The field animation can be found in Supporting Information. The incident Gaussian beam is emitted from the bottom. Several observations can be done from this set of data: (i) the slight standing-wave pattern on the input side (more noticeable in **Figure 4b** for sample III) at the center accounts for some reflection; (ii) the leaky wave supported by the hole array radiates in both the upward and downward directions; (iii) the output signal is composed of direct transmission through the illuminated holes along with the contribution from the upward

radiating leaky wave; hence, the transmission coefficient is higher than −3 dB; (iv) the leaky

wave involved in the EOT phenomenon is a negative space harmonic that enables the

backward phase propagation of the leaky wave on the structure. Considering the operation

frequency and the periodicity of the structure as well as the broadside radiation, it is easy to

demonstrate that it is the (0, −1) space harmonic, in good agreement with other structures that

also present enhanced transmission.[30],[32],[33],[35]-[37] From simulation and using a generalized

pencil-of-function method,[38] the leakage constant α normalized to the free-space wave vector

$k_0$ is estimated to be ~0.035 and ~0.015 for sample II and sample III at the corresponding

EOT frequency, which is in agreement with theory (i.e., leaky waves have a shorter

propagation length in dielectric-loaded subwavelength hole arrays than in freestanding

counterparts)[17] and is in the range observed in the analogous one-dimensional structure.[37]

The experimental results for sample III are shown in **Figure 5**, whereas simulations to track

the leaky wave mechanism described in the previous paragraph are plotted in Figure 4b. They

corroborate the previous results for sample II, underlining again the leaky wave mechanism

and, hence, the importance of large hole matrix size to achieve very high (total) transmission.

It is worth pointing out that transmission in sample II is in general larger except for the fully

perforated wafer illuminated with a collimated beam ($\varpi_0$ = 5 mm). The reason of this, perhaps,

unexpected result (due to the larger conductivity of copper and absence of dielectric loss) can

be traced to the above mentioned disparity between leakage constant for sample II and sample

III. The larger leakage constant, and thus shorter propagation length, implies stronger

coupling between the incident field and the leaky wave, resulting into a much smaller area

required to achieve EOT. When the total hole matrix is large enough compared to the

propagation length, transmission is then limited by conductive and dielectric losses. An

explanation from a different perspective can be found in the following section. Briefly, the

introduction of the dielectric slab makes the subwavelength hole array slightly more robust to

the angle of incidence (see **Figure 6 and 7**). Hence, the subwavelength hole array patterned

on PP is more robust (lower insertion loss) to tighter Gaussian beams that have broader angular spectrum than the freestanding counterpart. However, when the Gaussian beam is collimated and has a narrow angular spectrum, the insertion loss is mainly governed by the conductive and dielectric losses. Although polymers like PP have relative low absorption at THz frequencies,[39] the resonant nature of the transmission enhances the dielectric losses, penalizing gratings supported on substrates.

### 2.3. Gaussian beam angular spectrum dependence

In this final section, we perform a comprehensive analysis of the EOT hole arrays dependence on the characteristics of the incident Gaussian beam. The transmission coefficient for sample II and sample III fully perforated with subwavelength holes ($107 \times 107$ holes) under three different Gaussian beam illuminations ($\varpi_0 = 1$, 5 and 20 mm) is shown in Figure 6. The freestanding array (sample III) shows in general lower insertion loss at the resonant passband than the samples mounted on PP layers; this is primarily due to the removal of substrate reflections and dielectric losses. The insertion loss for the sample II and III is 0.18 and 0.04 dB, respectively. This result improves the insertion loss typically found in subwavelength hole arrays, [3],[6],[10],[15],[39]-[41] other resonant metasurfaces operating above 0.5 THz,[3],[42] and even nonresonant metasurfaces.[3],[42]-[44]

Gaussian beams can be represented by an infinite summation of plane waves with different angular wave vectors (angular distribution). So, the maximum transmission is smaller as the size of the Gaussian beam decreases because, even under normal incidence, a significant part of the beam impinges obliquely on the hole array (note that the incident wave vector is perpendicular to the surface only at the center axis of the beam and that the amplitude of the EOT resonance is reduced at oblique incidence, as discussed below with Figure 7).[45] Additionally, the null that appears before the onset of the grating lobe (see vertical arrow in Figure 6a,b) is known as Luebber's anomaly in the frequency selective surface (FSS)

9

literature.[46] This phenomenon is the responsible for the passband splitting observed in Figure 6, stronger for smaller beam-waist illuminations with a larger angular distribution.

To shed more light in the angular dependence, we analyse the simpler canonical problem using unit-cell simulations whereby the structure is infinite along $x$ and $y$, and is illuminated by a plane-wave (i.e., the illumination displays a single wave vector). The simulation results for sample II and III are shown in Figure 7 for both TE- and TM-polarized waves. One can notice that the null just below the onset of the diffraction lobe coined Luebber's anomaly in dielectric loaded FSSs also emerges for the freestanding sample. Such null is not preserved therefore in the substrate-based samples, but it is inherently bounded to the two-dimensional periodic nature of FSSs and the subwavelength hole array, and it emerges only for TM-polarized waves within our set of parameters.[45],[46]

## 3. Conclusion

To sum up, this manuscript has been devoted to grasp in detail the fundamentals of EOT. The requirement of a minimum number of illuminated holes to obtain a strong EOT resonance has been reviewed. It has been established clearly that the important parameter is the total number of holes rather than the illuminated area, demonstrating that there is a fundamental distinction between the number of illuminated holes and the total number of holes participating in the resonance process. This has been interpreted in terms of leaky waves excited thanks to the coupling of the incoming wave to the periodic structure $(0, -1)$ space harmonic, and subsequent coupling to radiation through the apertures. A direct parallelism has been found between hole arrays and small apertures on corrugated planes. The manuscript has also shown that freestanding resonant subwavelength hole arrays fabricated by electroforming display lower insertion losses under collimated illumination (i.e., quasi-plane-wave) than dielectric-loaded counterparts because of the avoidance of dielectric losses. The unprecedented minimum insertion loss reported here is 0.04 dB. In contrast, for focused Gaussian beams

with broad angular spectrum, hole arrays mounted on PP films surpass freestanding hole arrays because their spectral response is more stable against the angle of incidence. This manuscript gives the design guidelines to achieve high-performance quasi-optical filters for practical scenarios where there are sample area constraints or the incoming beam is not collimated. In this regard, other applications that can be greatly benefited from this study are vertical-cavity surface-emitting lasers[47] and surface-enhanced sensing platforms.[48]

**Experimental Section**

*Design and modelling*: The initial unit cell dimensions were calculated using a lossless equivalent circuit model[23],[29] and subsequently more accurately by means of a full-wave frequency-domain Floquet-mode simulation of the unit cell using the software CST Microwave Studio®. To reduce computational effort compared to a Drude model definition, a finite conductivity model for aluminum (Al) and copper (Cu) was used with $\sigma_{Al} = 3.56 \times 10^7$ S/m and $\sigma_{Cu} = 5.96 \times 10^7$ S/m, respectively. This approximation is valid given the still good conductivity of metals below 1 THz.[49] The polypropylene (PP) substrate produced by GoodFellow Company[50] was defined according to its measured material properties; further details of the PP's characterization can be found below. A tetrahedral mesh with minimum and maximum edge length of 0.08 μm and 129.01 μm was used. A schematic diagram of the sample with the geometrical parameters can be found in Figure 1.

To a good approximation, the incoming THz beam in all experimental setups has a linearly wavelength dependent Gaussian profile with certain beam-waist that can be either smaller, similar or larger than the hole matrix. Hence, in order to achieve a reliable full-wave simulation of the actual measurement, the transient solver of CST Microwave Studio® was used. The whole Ø50 mm wafer (as shown in the bottom panel of Figure 1) was modelled and the THz beams of different beam-waist, according to the experimental setup, were modelled with the solver-implemented Gaussian beam defined at 0.6 THz to have the focus exactly on

11

the sample surface. The temporal Gaussian signal of the spatial Gaussian beam has spectral components only between 0.4 and 0.7 THz to alleviate computational effort. Boundary conditions were set to the software-defined open (add space), i.e., perfectly matched layers, to model the wafer embedded in free-space. Given the twofold symmetry of the problem, a horizontal $y = 0$ electric and a vertical $x = 0$ magnetic mirror planes are applied to consider only a quarter of the simulation box. In this case, a non-uniform hexahedral mesh with smallest and largest cell edge of 2.5 μm and 42.6 μm, respectively, was used. The residual energy in the calculation volume is $1 \times 10^{-6}$ (−60 dB) of its peak value.

*Fabrication and measurements setups*: Three independent methods to determine the dielectric permittivity of PP films were used: Mach-Zehnder interferometry, Fabry-Perot interferometry and "supplementary FSS" method (whereby a FSS with cross-shaped metallic elements was patterned on the PP substrate and full-wave simulations were fitted to the experimental data). A THz backward wave oscillator (BWO) and a Golay-cell detector[51]-[53] were employed for PP characterization . The average dielectric permittivity is $< \varepsilon_r > = 2.251 \pm 0.011$ and the loss tangent is estimated to be $\tan\delta \leq 10^{-3}$ within the above-mentioned bandwidth, which is consistent with previously published results.[39]-[41],[51] The comparative results using the different characterization methods will be reported elsewhere.

To create a high-quality micropattern of the EOT arrays investigated in this work, a contact photolithography technique adapted for flexible substrates[39],[41] was used for PP-backed samples, whereas a combination of photolithographic and electroplating technologies[52],[53] was employed for the freestanding samples.

After fabrication, the samples were characterized with four different high-resolution THz instruments:

1. ABmm$^{TM}$ millimeter-wave vector network analyzer.[54] The spectral resolution was 0.75 GHz and the beam-waist in this setup was estimated to be ~3 mm for focused

illumination (achieved by means of ellipsoidal mirrors) at 0.22 THz. This instrument was used for rectangular-lattice subwavelength hole arrays only.

2. Quasi-optical continuous-wave (CW) BWO spectrometer. In this instrument the THz signal was measured with a lock-in Golay-cell detector operating at the modulation frequency of 23 Hz specified by a mechanical obturator (beam chopper).[51]-[53] The spectral resolution was 50 MHz and the beam-waist in this setup was estimated to be ~10 mm. To minimize standing waves in the free-space path formed due to coherent CW illumination, samples were slightly tilted (~1 deg) with respect to the incident THz beam. The BWO spectrometer was utilized only for the rectangular-lattice hole arrays of the largest size ($107 \times 107$ holes).

3. TERA K15 all fiber-coupled THz time-domain spectrometer from Menlo Systems.[55] The lock-in time constant was set to 300 ms and the total scan length was 208 ps (in the results of Fig. 3) or 104 ps (in the rest of figures) to have a spectral resolution of 4.8 and 9.6 GHz, respectively. At the sample position, the beam-waist diameter of the THz beam was estimated with the help of a continuously variable iris diaphragm to be 5 mm at 0.6 THz. By placing TPX plano-convex lenses of effective local length ~54 mm in the free-space path, the beam-waist at the sample position was reduced to 1 mm.

4. TPS Spectra 3000 from Teraview.[56] The free-space path was purged with nitrogen and an average representation of the transmission coefficient was obtained with 100 single measurements. An apodization window was applied to the waveforms, resulting into a 6 GHz frequency resolution. The beam-waist in this setup was estimated to be ~1.5 mm at 0.6 THz.[57]

**Supporting Information**
Supporting Information is available from the Wiley Online Library or from the author.

<div align="right">

Received: ((will be filled in by the editorial staff))
Revised: ((will be filled in by the editorial staff))
Published online: ((will be filled in by the editorial staff))

</div>

References

[1]     T. Xu, H. Shi, H., Y.-K. Wu, A. F. Kaplan, J. G. Ok, L. J. Guo, *Small* **2011**, *7*, 3128.

[2]     M.-C. Estevez, M. A. Otte, B. Sepulveda, L. M. Lechuga, *Anal. Chim. Acta* **2014**, *806*, 55.

[3]     S. B. Glybovski, S. A. Tretyakov, P. A. Belov, Y. S. Kivshar, C. R. Simovski, *Phys. Rep.* **2016**, *634*, 1.

[4]     T. Matsui, A. Agrawal, A. Nahata, Z. Valy Vardeny, *Nature* **2007**, *446*, 517.

[5]     T. Thio, H. F. Ghaemi, H. J. Lezec, P. A. Wolf, T. W. Ebbesen, *J. Opt. Soc. Am. B* **1999**, *16*, 1743.

[6]     F. Miyamaru, M. Hangyo, *Appl. Phys. Lett.* **2004**, *84*, 2742.

[7]     M. Beruete, M. Sorolla, I. Campillo, J. S. Dolado, *IEEE Microw. Wireless Compon. Lett.* **2005**, *15*, 116.

[8]     J. Bravo-Abad, A. Degiron, F. Przybilla, C. Genet, F. J. García-Vidal, L. Martín-Moreno, T. W. Ebbesen, *Nat. Phys.* **2006**, *2*, 120.

[9]     F. Przybilla, A. Degiron, C. Genet, T. W. Ebbesen, F. de León Pérez, J. Bravo-Abad, F. J. García-Vidal, L. Martín-Moreno, *Opt. Express* **2008**, *16*, 9571.

[10]    H. Cao, A. Nahata, *Opt. Express* **2004**, *12*, 3664.

[11]    M. Beruete, M. Sorolla, I. Campillo, J. S. Dolado, L. Martín-Moreno, J. Bravo-Abad, F. J. García-Vidal, *Opt. Lett.* **2004**, *29*, 2500.

[12] R. Gordon, *Phys. Rev. A* **2007**, *76*, 053806.

[13] M. Navarro-Cía, M. Beruete, M. Sorolla, *Metamaterials* **2011**, *5*, 125.

[14] M. Beruete, M. Navarro-Cía, V. Torres, M. Sorolla, *Phys. Rev. B* **2011**, *84*, 075140.

[15] Y. Yang, D. R. Grischkowsky, *IEEE Trans. Terahertz Sci. Technol.* **2013**, *3*, 151.

[16] J. B. Pendry, L. Martín-Moreno, F. J. García-Vidal, *Science* **2004**, *305*, 847.

[17] V. Lomakin, E. Michielssen, *Phys. Rev. B* **2005**, *71*, 235117.

[18] C. Genet, T. W. Ebbesen, *Nature* **2007**, *445*, 39.

[19] E. Hendry, A.P. Hibbins, J.R. Sambles, *Phys. Rev. B* **2008**, *78*, 235426.

[20] H. Liu, P. Lalanne, *Nature* **2008**, *452*, 728.

[21] A. Bitzer, M. Nagel, *Appl. Phys. Lett.* **2008**, *92*, 231101.

[22] F. J. García-Vidal, L. Martín-Moreno, T. W. Ebbesen, L. Kuipers, *Rev. Mod. Phys.* **2010**, *82*, 729.

[23] M. Beruete, M. Navarro-Cía, M. Sorolla, *IEEE Trans. Microwave Theory Tech.* **2011**, *59*, 2180.

[24] H. J. Lezec, T. Thio, *Opt. Express* **2004**, *12*, 3629.

[25] A. Hessel, A. A. Oliner, *Appl. Opt.* **1965**, *4*, 1275.

[26] R. Ulrich, presented at the Symposium on Optical and Acoustical Micro-Electronics, New York, N.Y., April 16-18, 1974. (A76-10201 01-33) Brooklyn, N.Y., Polytechnic Press of the Polytechnic Institute of New York, 1975, 359-376.

[27] A. Ishimaru, *Electromagnetic Wave Propagation, Radiation, and Scattering*, Prentice Hall, NJ, USA **1991**.

[28] L. Martin-Moreno, F. J. Garcia-Vidal, H. J. Lezec, K. M. Pellerin, T. Thio, J. B. Pendry, T. W. Ebbesen, *Phys. Rev. Lett.* **2001**, *86*, 1114.

[29] F. Medina, F. Mesa, R. Marqués, *IEEE Trans. Microwave Theory Tech.* **2008**, *56*, 3108.

[30] D. R. Jackson, A. A. Oliner, T. Zhao, J. T. Williams, *Radio Sci.* **2005**, *40*, 1.

[31]    M. Beruete, M. Sorolla, M. Navarro-Cía, F. Falcone, I. Campillo, V. Lomakin, *Opt. Express* **2007**, *15*, 1107.

[32]    H. J. Lezec, A. Degiron, E. Devaux, R. A. Linke, L. Martín-Moreno, F. J. García-Vidal, T. W. Ebbesen, *Science* **2002**, *297*, 820.

[33]    M. Beruete, M. Sorolla, I. Campillo, J. S. Dolado, *IEEE Microwave Wireless Compon. Lett.* **2005**, *15*, 286.

[34]    M. Camacho, R. R. Boix, F. Medina, *Phys. Rev. E* **2016**, *93*, 063312.

[35]    M. Beruete, I. Campillo, J. S. Dolado, E. Perea, F. Falcone, M. Sorolla, *IEEE Antennas Wireless Propag. Lett.* **2005**, *4*, 365.

[36]    U. Beaskoetxea, M. Navarro-Cía, M. Beruete, *J. Phys. D: Appl. Phys.* **2016**, *49*, 265103.

[37]    U. Beaskoetxea, S. Maci, M. Navarro-Cía, M. Beruete, *IEEE Trans. Antennas Propag.* **2017**, *65*, 17.

[38]    Y. Hua, T. K. Sarkar, *IEEE Trans. Antennas Propag.* **1989**, *37*, 229.

[39]    M. Navarro-Cía, S. A. Kuznetsov, M. Aznabet, M. Beruete, F. Falcone, M. Sorolla Ayza, *IEEE J. Quantum Electron.* **2011**, *47*, 375.

[40]    S. A. Kuznetsov, M. Navarro-Cía, V. V. Kubarev, A. V. Gelfand, M. Beruete, I. Campillo, M. Sorolla, *Opt. Express* **2009**, *17*, 11730.

[41]    M. Aznabet, M. Navarro-Cía, S. A. Kuznetsov, A. V. Gelfand, N. I. Fedorinina, Yu. G. Goncharov, M. Beruete, O. El Mrabet, M. Sorolla, *Opt. Express* **2008**, *16*, 18312.

[42]    I. Al-Naib, W. Withayachumnankul, *J. Infrared, Millimeter, Terahertz Waves* **2017**, *38*, 1067.

[43]    M. Pu, X. Li, X. Ma, Y. Wang, Z. Zhao, C. Wang, C. Hu, P. Gao, C. Huang, H. Ren, X. Li, F. Qin, J. Yang, M. Gu, M. Hong and X. Luo, *Science Adv.* **2015**, *1*, e1500396.

[44]    D. Tang, C. Wang, Z. Zhao, Y. Wang, M. Pu, X. Li, P. Gao, X. Luo, *Laser Photonics Rev.* **2015**, *9*, 713.

[45]    P. Rodríguez-Ulibarri, M. Navarro-Cía, R. Rodríguez-Berral, F. Mesa, F. Medina, M. Beruete, Annular Apertures in Metallic Screens as Extraordinary Transmission and Frequency Selective Surface Structures, *IEEE Trans. Microwave Theor. Tech.* **2017**, *65*, 4933.

[46]    R. J. Luebbers, B. A. Munk, *IEEE Trans. Antennas Propag.* **1978**, *AP-26*, 536.

[47]    T. Onishi, T. Tanigawa, T. Ueda, D. Ueda, *IEEE J. Quantum Electron.* **2007**, *43*, 1123.

[48]    R. Gordon, A. G. Brolo, D. Sinton, K. L. Kavanagh, *Laser Photonics Rev.* **2009**, *4*, 311.

[49]    M. Naftaly, in *Terahertz Metrology*, (Ed: M. Naftaly), Artech House, Boston, MA, USA, **2015**, Chap. 9, pp. 251-281.

[50]    http://www.goodfellow.com/, accessed: November 2017

[51]    S. A. Kuznetsov, A. G. Paulish, M. Navarro-Cía, A. V. Arzhannikov, *Sci. Rep.* **2016**, *6*, 21709.

[52]    M. K. A. Thumm A. V. Arzhannikov, V. T. Astrelin, A.V. Burdakov, N. S. Ginzburg, I. A. Ivanov, P. V. Kalinin, S. A. Kuznetsov, M. A. Makarov, K. I. Mekler, A.G. Paulish, N. Yu. Peskov, S. V. Polosatkin, S.A. Popov, V. V. Postupaev, A. F. Rovenskikh, A. S. Sergeev, S. L. Sinitsky, V. F. Sklyarov, V. D. Stepanov, L. N. Vyacheslavov, V. Yu. Zaslavsky, *Int. J. Terahertz Sci. Techn.* **2012**, *5*, 18.

[53]    S. A. Kuznetsov, M. A. Astafyev, A. V. Gelfand, A. V. Arzhannikov, in Proc. 44th Eur. Microw. Conf. (EuMC 2014), Rome, Italy, 2014, pp. 881–884.

[54]    http://www.abmillimetre.com/, accessed: November 2017

[55]    http://www.menlosystems.com/products/thz-time-domain-solutions/all-fiber-coupled-terahertz-spectrometer/, accessed: November, 2017

[56]    http://www.teraview.com/, accessed: November, 2017

[57]    J. B. Sleiman, Ph.D. thesis, Université de Bordeaux, **2016**.
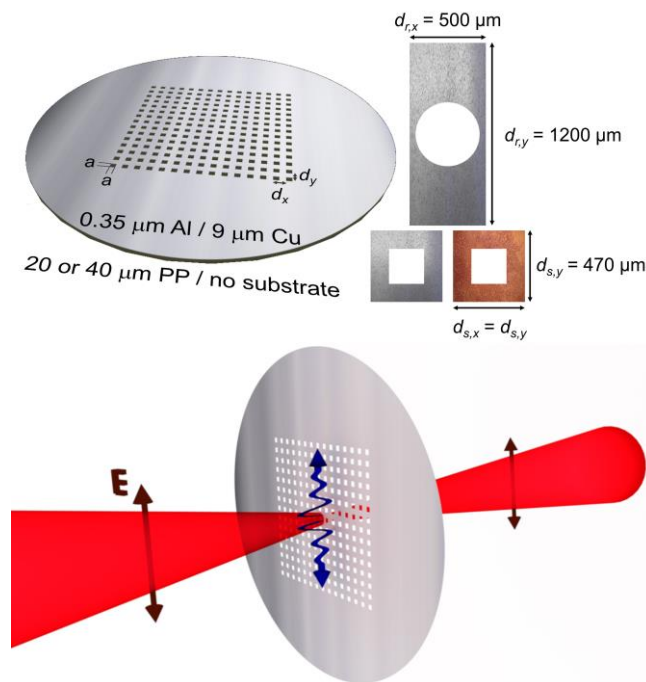
**Figure 1.** (top left) Schematic diagram of the subwavelength hole array in a square lattice. The metal thickness is 0.35 µm and 9 µm for the Al and Cu samples, respectively. The Al sample is patterned on a 20 µm or 40 µm thick PP film, whereas the Cu sample is freestanding. The overall diameter of the sample is 50 mm in all cases. The sample lies in the *xy* plane with the linearly-polarized THz beam incident in the *z*-direction either focused or collimated. (top right) Unit cells of the circular hole array in a rectangular lattice with hole diameter $a_r = 420$ µm and lattice constants $d_{r,x} = 500$ µm, $d_{r,y} = 1200$ µm –top– and the square hole array in a square lattice with $d_{s,x} = d_{s,y} = 470$ µm and aperture side $a_s = 230$ µm –bottom–. (bottom) Schematic diagram of the experimental setups.
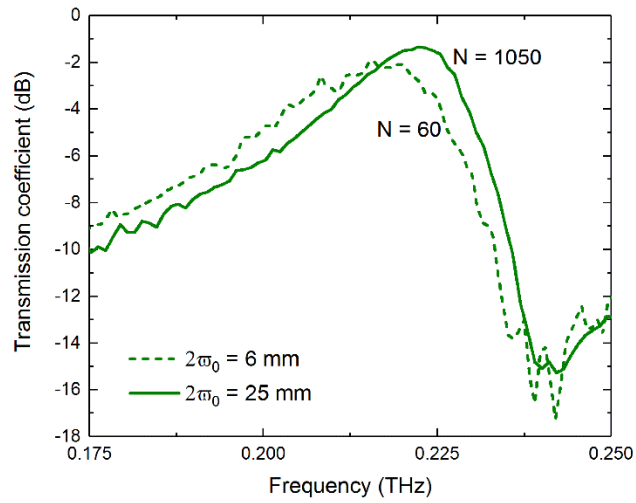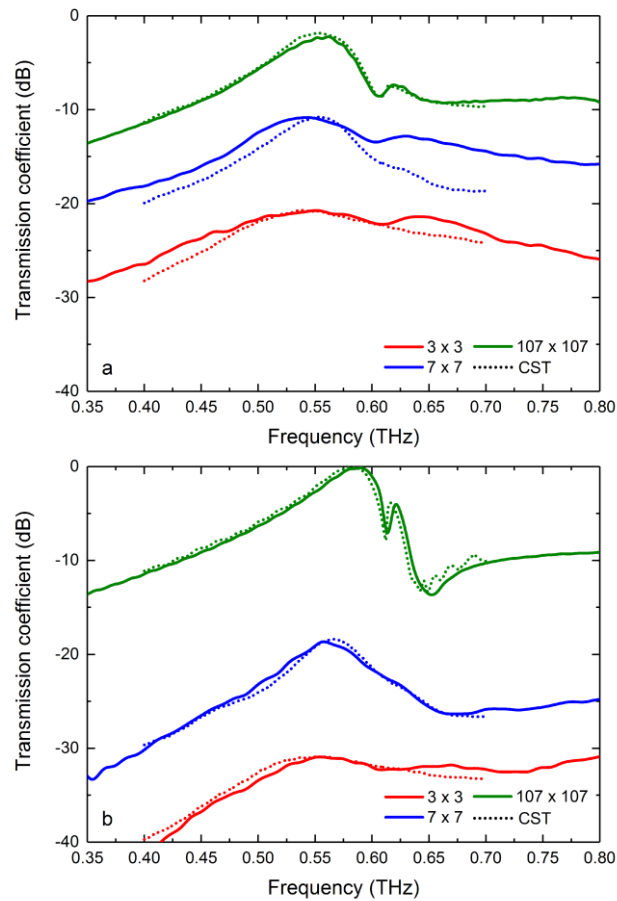
**Figure 2.** Measured transmission coefficient for sample I at different beam spot sizes ($2\varpi_0$ is the beam diameter).
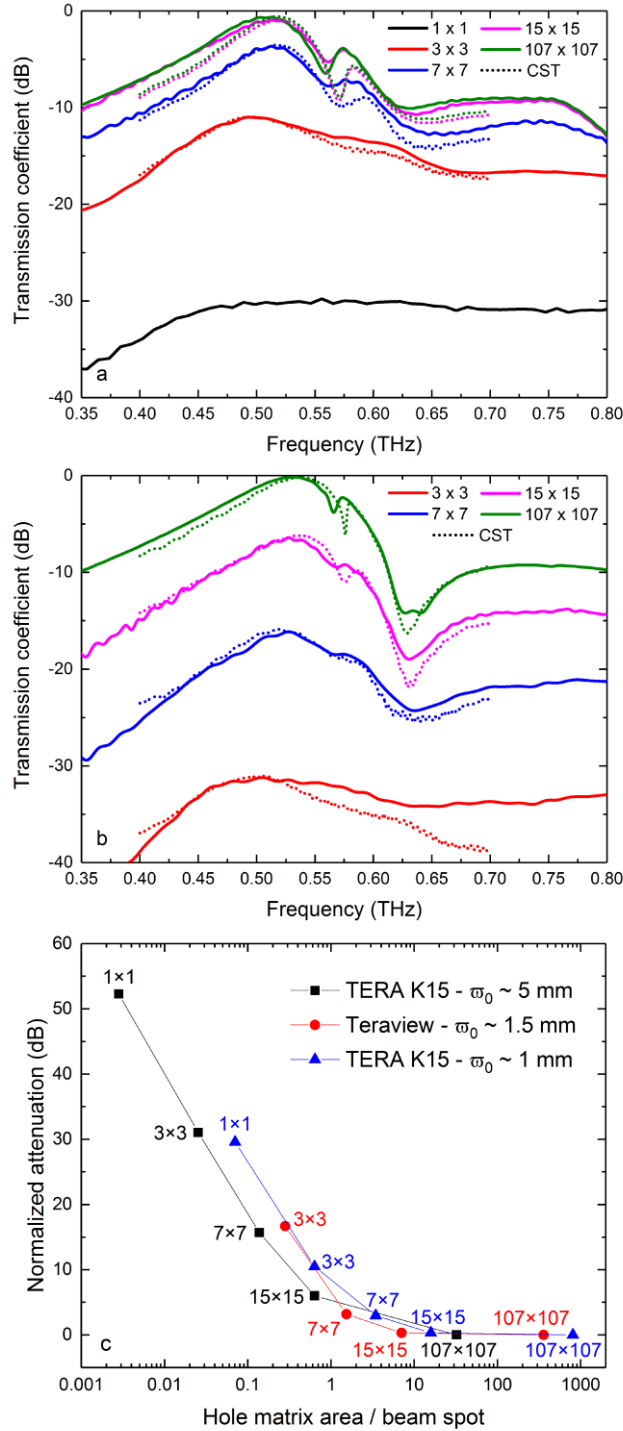
**Figure 3.** Measured (solid lines) and calculated spectral transmittance (short-dashed lines) of sample II having the different number of holes upon illumination by (a) a $\varpi_0 = 1$ mm focused beam and (b) a $\varpi_0 = 5$ mm collimated beam. (c) Measured attenuation of EOT peak with respect to the 107×107 holes sample as a function of the hole matrix area normalized to the beam spot (i.e., $n_x \cdot d_x \cdot n_y \cdot d_x / (\pi \cdot \varpi_0^2)$) for three different beam-waists.
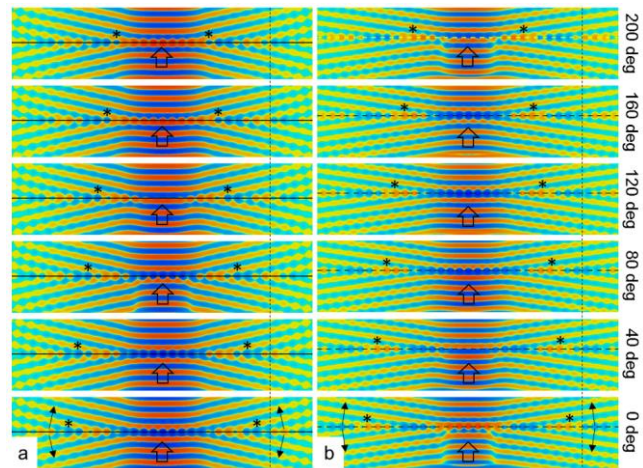
**Figure 4.** Normalized electric field $E_x(x, z)$ at (a) 0.51 THz – sample II –, and (b) 0.55 THz – ample III –. From the bottom up: phase 0, 40, 80, 120, 160, and 200 deg. To guide the eye, a vertical dashed line is included in each panel together with two asterisk, tilted arrows and vertical arrows that enable to track the phase evolution of the leaky waves, the leakage direction and the incident beam, respectively.

**Figure 5.** Measured (solid lines) and calculated spectral transmittance (short-dashed lines) of sample III having the different number of holes illuminated by (a) a 1 mm beam-waist focused and (b) a 5 mm beam-waist collimated beam.
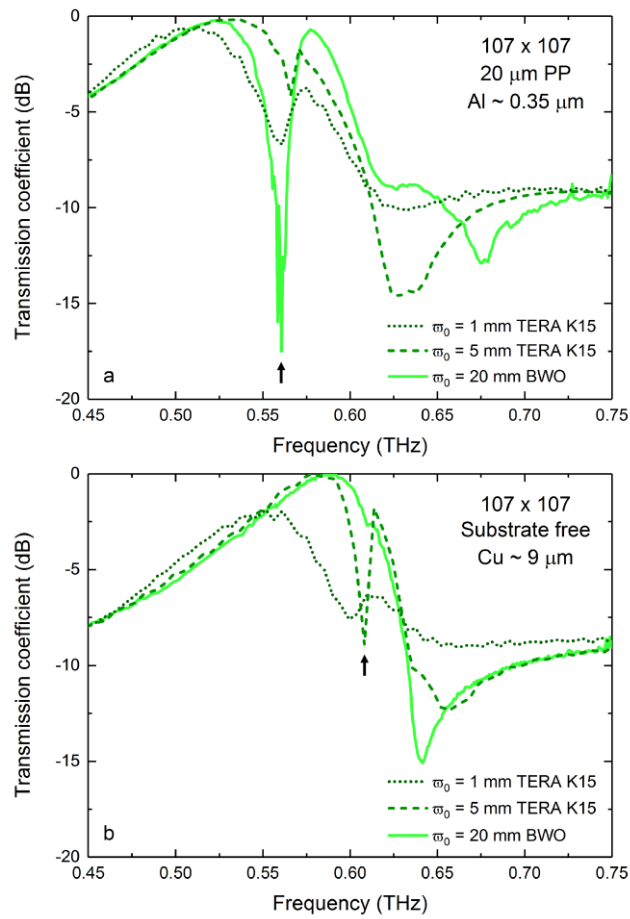
**Figure 6.** Measured transmission spectra for (a) sample II and (b) sample III with $107 \times 107$ holes illuminated with THz beams of different beam-waists: 1 mm, 5 mm and 20 mm.
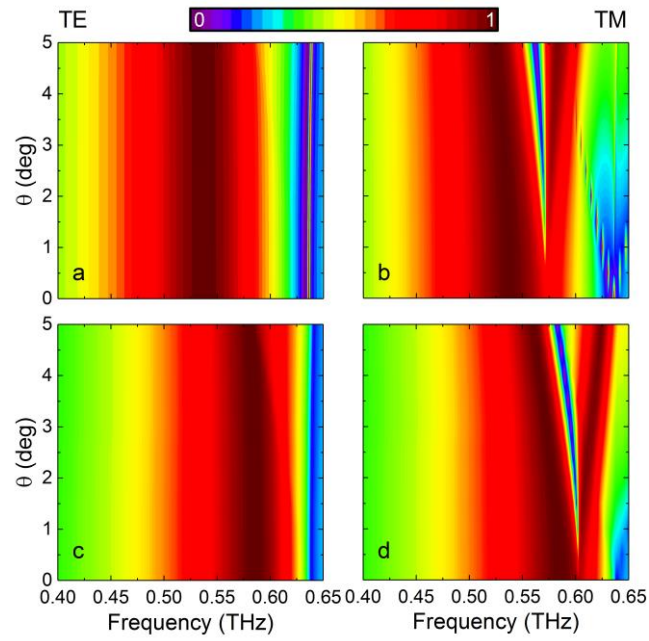
**Figure 7.** Calculated transmission coefficient in linear scale for (a, b) sample II and (c, d) sample III under oblique incidence – with azimuthal angle φ = 0 – for (a, c) TE- and TM-polarized waves (b, d).

**Table I.** Sample labels, geometrical parameters and corresponding EOT resonance frequency under plane-wave illumination

| Sample | $d_x$ (μm) | $d_y$ (μm) | $a$ (μm) | PP thickness (μm) | Metal thickness (μm) | EOT resonance (THz) |
|---|---|---|---|---|---|---|
| Rectangular-lattice | | | | | | |
| I | 500 | 1200 | 420 | 40 | 0.35 Al | ~ 0.22 |
| Square-lattice | | | | | | |
| II | 470 | 470 | 230 | 20 | 0.35 Al | ~ 0.53 |
| III | 470 | 470 | 230 | 0 | 9 Cu | ~ 0.58 |

**Table of content: Efficient extraordinary optical transmission though subwavelength apertures have been the preserve of large arrays under expanded beam illumination.** Recognizing the key role played by leaky waves, high transmission is obtained here with a reduced illumination spot when there are sufficient number of lateral holes out of the illumination spot for the leaky waves to mediate. This has strong implications for applications.

**Keyword** extraordinary transmission, leaky wave mode, terahertz, time-domain spectroscopy, continuous-wave spectroscopy

Miguel Navarro-Cía*, Víctor Pacheco-Peña, Sergei A. Kuznetsov, and Miguel Beruete*

**Extraordinary THz Transmission with a Small Beam Spot: the Leaky Wave Mechanism**

ToC figure